The 7 May 2001 induced seismic event in the Ekofisk oil field, North Sea

L. Ottemöller,[1] H. H. Nielsen,[2] K. Atakan,[3] J. Braunmiller,[4] and J. Havskov[3]

[1] A moderate size seismic event on 7 May 2001 was strongly felt on platforms in the Ekofisk oil field, in the southern North Sea, but did not cause damage to platforms or wells. We combined near- and far-field observations to develop a consistent source model and to determine whether the event was induced. Seismic data placed the epicenter inside the Ekofisk field and suggested a shallow source depth based on spectral and moment tensor analysis. GPS data from the Ekofisk platforms displayed permanent vertical and horizontal movement due to the event. A topographic bulge in the sea bottom, revealed by differential bathymetry data, and overpressure in the overburden in the northeastern part of the field, detected only after the event, had been caused by unintentional water injection that started in 1999. The injection pressure and rate were sufficient to raise the overburden. Pressure gauge and compaction data ruled out that the event occurred at reservoir level, which was further supported by unaffected production rates and absence of well failure. We therefore conclude that the event occurred in the overburden, at less than 3 km depth. Initially, this appeared unlikely on account of very low shear strength of the overburden clay-rich shale and mud rocks. The seismic event was induced owing to stress changes caused by water injection. The event possibly initiated on the northern flank of the field near the water injector and may have involved flexure of the overburden into the depression bowl in the rest of the field. Moment tensor analysis is consistent with a pure double-couple source. We suggest that slip occurred on the near-horizontal rather than along the near-vertical nodal plane. Stress drop was low, and owing to the low overburden shear strength, the event released less energy than a typical stress drop event with similar source dimensions.

1. Introduction

[2] On 7 May 2001 at 0943 UT, a seismic event of moderate size ($M_w = 4.1–4.4$) occurred in the southern North Sea. The event was strongly felt on platforms and associated structures within the Ekofisk oil field as ten seconds swaying and trembling. Initial locations placed the event in the vicinity of the Ekofisk oil field. The location uncertainties, however, were so large that the event could have also occurred inside the field. This, combined with the severe shaking on the platforms, caused the operator of the Ekofisk field, ConocoPhillips Norway, to ask the University of Bergen as operator of the Norwegian National Seismic Network, to perform a detailed seismic data analysis [*Atakan et al.*, 2001; J. Braunmiller et al., The May 7, 2001 earthquake in the Ekofisk area, North Sea, *Orfeus Electronic Newsletter*, *3*(2), 2001, available at http://www.orfeus-eu.org/newsletter/vol3no2/ekofisk.html]. As more data were analyzed, the computed epicenter location moved into the Ekofisk field.

[3] Seismic recordings were available only from the far field. With these, we attempted to resolve epicenter location, source depth and mechanism. Macroseismic information on how the event had been felt on the platforms was collected. Additional near-field measurements on the structures in the Ekofisk field included GPS, interplatform distance, pressure and tide gauge observations. The GPS data confirmed the event location within the outline of the Ekofisk field. A bathymetric survey carried out two months after the event was compared with 1999 measurements, allowing the construction of a differential bathymetry map. Differential bathymetry and unusual pressure data from the northern flank of the field hinted at the possibility of the seismic event being induced. A seismic survey was done in 2003 and compared to a previous survey in 1999.

[4] This paper links the seismic far-field observations with the various nonseismic near-field measurements from the Ekofisk field. On the basis of these observations, we present a model for the processes leading to the seismic event and discuss a plausible source scenario. Our multi-

---

[1]British Geological Survey, Edinburgh, UK.
[2]ConocoPhillips, Tananger, Norway.
[3]Department of Earth Science, University of Bergen, Bergen, Norway.
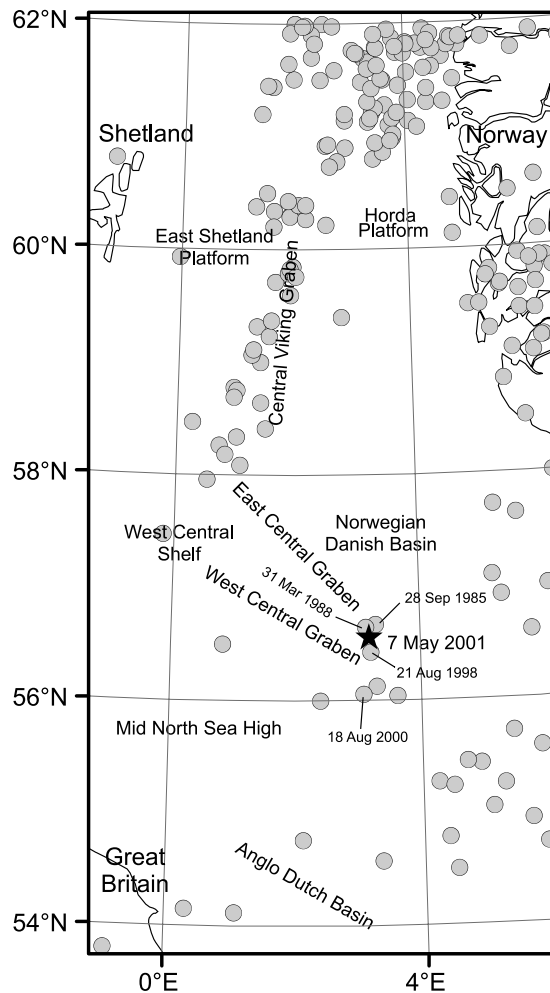[4]Swiss Seismological Service, ETH-Hoenggerberg, Zurich, Switzerland.

Figure 1. Regional tectonic features and seismicity (circles, same size for all magnitudes) with $M \geq 2.5$ merged from University of Bergen, British Geological Survey, and International Seismological Centre catalogues for the period 1970–2003. The epicenter of the 7 May 2001 event is indicated by a star. Four further events in the vicinity of Ekofisk are labeled.

disciplinary case study aims to establish whether the seismic event was induced.

2. Background

2.1. Tectonic Setting and Seismicity

[5] The Ekofisk field is located within the Central Graben in the southern North Sea (Figures 1 and 2). The Central Graben is a NW-SE fault-bounded trough that was initiated during a major rifting period in the Late Triassic, with crustal extension continuing through Jurassic times [*Pekot and Gersib*, 1987]. The Ekofisk reservoir, which lies about 3000 m below the seafloor, is a salt-induced, roughly elliptical anticline structure that is 11.2 km long (N-S) and 5.4 km wide (E-W). The Ekofisk and Tor formations at the top of the 800 m chalk group contain the productive intervals (Figure 3). The overburden consists largely of very fine grained, mechanically weak, clay-rich shales and mud rocks. These rocks are overpressured (above

hydrostatic) from ~1100 m downward due to rapid sedimentation and exert a vertical stress of ~9000 psi (62 MPa) on the reservoir. The overburden load on the reservoir is supported jointly by the overpressured reservoir fluids initially at >7000 psi (48 MPa) at the top of the reservoir and the matrix of the porous chalk.

[6] During its geological development, the Ekofisk structure has been affected by numerous episodes of movement and the reservoir is naturally fractured, facilitating hydrocarbon extraction. Both the uppermost overburden (top 1100 m) and the deeper overburden are faulted [*Nagel and Strachan*, 1998]. The vertical extent of faults in the deeper overburden can reach up to 1 km. In the upper overburden faulting is laterally extensive, but vertical fault dimensions are less than 50 m [*Nagel*, 1998]. Fault orientation in the deeper overburden are generally NE-SW or NW-SE.

[7] Seismicity rates in Norway and the nearby continental shelf areas are low to intermediate [*Bungum et al.*, 1991]. In southwestern Norway, most seismic events are located in the Norwegian Danish Basin and the coastal areas between 56°N and 63°N (Figure 1). The Viking Graben appears seismically more active than the Central Graben with respect to both event size and frequency. The largest event in either graben was the 1927 M_s = 5.3 earthquake in the Viking Graben [*Bungum et al.*, 1991]. The regional stress pattern is dominated by the Mid-Atlantic Ridge push force [*Bungum et al.*, 1991; *Hicks et al.*, 2000]. *Grollimund et al.* [2001] showed that in the Central Graben maximum horizontal stresses are in NNW-SSE direction, which is
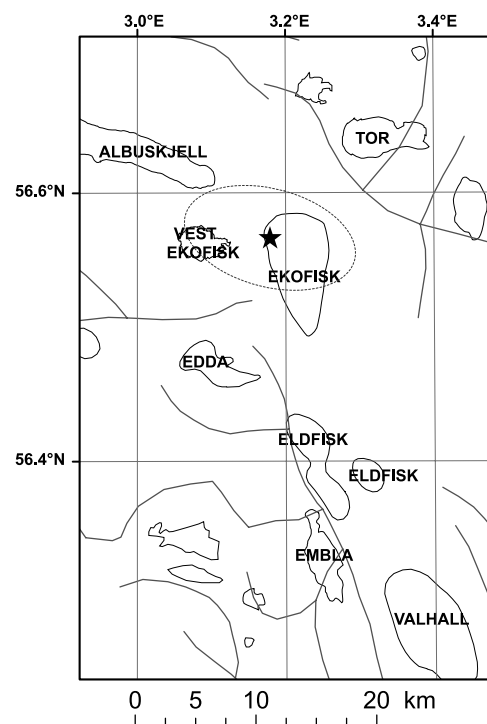

Figure 2. Outline of the Ekofisk and neighboring fields and fault lines (data provided by the Norwegian Petroleum Directorate, 2004). The epicenter of the 7 May 2001 event is indicated by a star. The dotted line gives the 90% confidence error ellipse.
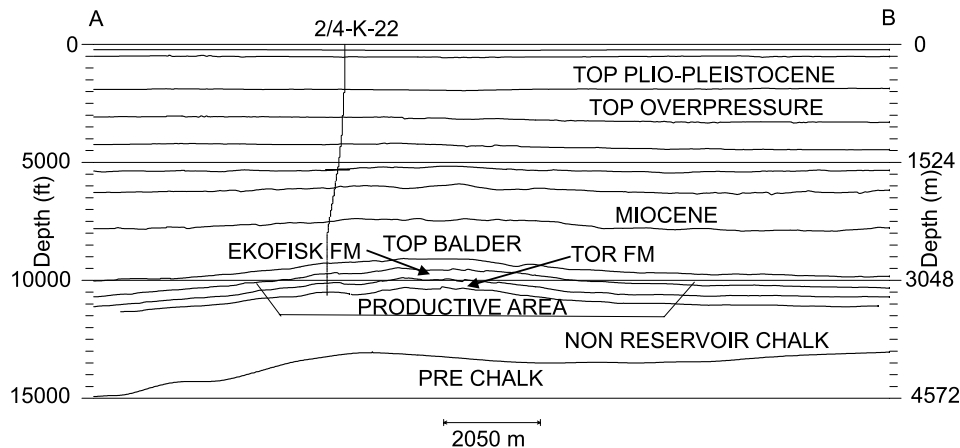
Figure 3. Section in N-S direction across the Ekofisk field. The Ekofisk and Tor formations (FM) are the productive layers. The projected well path of 2/4-K-22 is also shown.

expected to result in strike-slip or reverse faulting. Since 1970, few earthquakes have been located by the land-based seismic networks in the vicinity of the Ekofisk field (Figure 1). Epicenter uncertainties of events in this area, based on the arrival times of seismic waves, are about 15 km horizontally [*Bungum et al.*, 1991]. Prior to the 2001 event, the 1988 $M_L = 2.5$ event was the only event felt at the Ekofisk platforms [*Macbeth*, 1988].

2.2. Ekofisk Production History

[8] Ekofisk, discovered in 1969, is the largest chalk field in the North Sea [*Pekot and Gersib*, 1987; *Kvendseth*, 1988]. Production on the giant Ekofisk oilfield started in July 1971. Initially, the hydrocarbon recovery was achieved by natural depletion from 4 wells. Extensive development began with the commitment to permanent structures in 1972. Currently the field is developed with 71 producing wells, 38 water injection wells and 3 gas injection wells located on 4 producing platforms and 2 water injection platforms. Gas and water injection were implemented as secondary recovery methods. Production has risen continuously as a result of the water injection and redevelopment. The Ekofisk field production, with 17.2×10^6 m^3 oil and 2.7×10^9 m^3 gas/yr (figures published by the Norwegian Petroleum Directorate, 2004), is presently close to the initial production level, more than 30 years after production started. Injection of drill cuttings into the overburden started in 1996, after extensive risk and cost evaluation [*Nagel and Strachan*, 1998].

2.3. Reservoir Compaction and Subsidence

[9] During the natural depletion phase (before 1988), fluid removal from the reservoir reduced the pore pressure and increased the effective stress within the chalk. As a result of the increased effective stress, the reservoir chalk has compacted. Before production started, the overburden was in pore pressure equilibrium with the reservoir. The reservoir pressure depletion did not create any significant depletion of the overburden.

[10] The overburden consists of undercompacted weak shale and mud rocks and thus the compaction is transferred almost instantaneously to the seafloor as subsidence [*Nagel*, 2001; *Chin and Nagel*, 2004]. Overburden bridging effects

may have taken place, resulting in a volume of seafloor subsidence less than the reservoir compaction volumes [*Hettema et al.*, 2002]. In 1984, subsidence of 3 m, with a rate of 0.4 m/yr, was discovered in the Ekofisk field [*Nagel*, 1998; *Sylte et al.*, 1999]. In August 2002, the total subsidence at the Ekofisk crest had reached 8.26 m. At present, the subsidence rate is 0.1–0.15 m/yr and thus significantly lower than previously.

[11] The current, reduced subsidence rate was achieved through water injection starting in 1987, which led to reservoir repressurization. The Ekofisk water flood was expanded in 1992, injection volumes doubled and at present are 700,000 barrels/d (112,000 m^3/d). The current water injection rate is higher than off-take rates resulting in a field-wide repressurization.

2.4. Induced Seismicity

[12] Earthquakes are either tectonic, triggered or induced. Here, we consider triggered and induced events as those related to human activity, such as construction of water reservoirs and hydrocarbon production [*Gupta and Chadha*, 1995; *Scholz*, 2002]. Triggered events would occur without human activity though later in time, while induced events are caused solely by human activity.

[13] Induced seismicity at hydrocarbon producing sites has been attributed to injection [*Raleigh et al.*, 1972] and subsidence [*Kovach*, 1974; *Yerkes and Castle*, 1976]. *Grasso* [1992] presented three mechanisms capable of giving rise to induced and triggered events. First, increased pore pressure due to injection decreases normal stresses and thus fracture occurs following the Coulomb criterion [*Scholz*, 2002]. This mechanism causes seismic slip within the reservoir, typically with magnitudes $M_L \leq 3$. Second, fluid withdrawal causes a change in pore pressure, which causes changes in the geological structure. Stress changes are transferred to the area immediately surrounding the reservoir, where seismic events, typically with $M_L \leq 5$ can occur. *Segall* [1989] investigated the stress changes inside a poroelastic medium undergoing fluid extraction and explained how extraction may promote fault slip. Modeled stress changes predict increased horizontal compression below and above the reservoir leading to reverse faulting, and decreased horizontal stresses on the flanks leading to
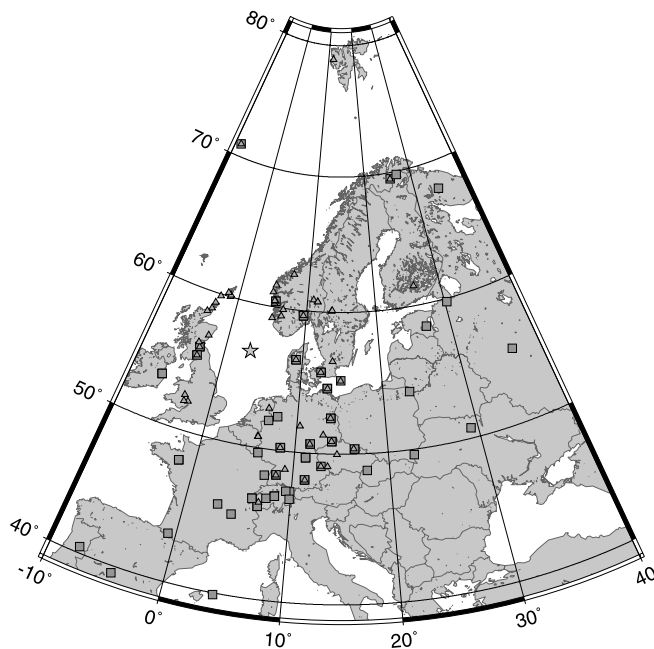
Figure 4. Map of seismic stations used for analyzing the 7 May 2001 event. The epicenter is given by a star, squares show stations used for moment tensor inversion, and triangles give stations used in epicenter determination.

normal faulting. Third, earthquakes can be caused by massive load removal during hydrocarbon extraction. These events are seen as crustal adjustments to stress pattern changes.

[14] There are numerous examples of induced seismicity [e.g., *Grasso*, 1992; *Segall*, 1989]. Possibly the largest triggered/induced events ($M_s \geq 7$) occurred 1976 and 1984 in the Gazli field area, Uzbekistan. *Kovach* [1974] described subsidence related earthquakes at the Wilmington oil field, California, which took place between 1947 and 1961. Between 1983 and 1987, three events in California ($M = 5.9–6.5$) were considered to be related to hydrocarbon production [*Segall*, 1985; *McGarr*, 1991]. Recently, *Gomberg and Wolf* [1999] discussed the relationship between the 1997 $M_w = 4.9$ southern Alabama earthquake and hydrocarbon production.

[15] Because of a lack of nearby stations, it has not been possible to determine whether events near the Ekofisk field were induced. Therefore subsidence at Ekofisk before 2001 is considered aseismic, by which we mean that adjustments in the overburden were not detected by any seismograph network. However, casing deformation in the overburden suggested that near-horizontal shearing had occurred [*Nagel*, 1998]. During an 18-day monitoring period in 1997, microseismic activity (1800 events with $M \leq -1$) was detected from an observation well [*Maxwell et al.*, 1998; *Maxwell and Urbancic*, 2001]. Most events occurred in the upper part of the reservoir and were attributed to induced deformation. The few event locations above the reservoir were considered unreliable. This type of induced activity falls into the first category [*Grasso*, 1992]. The microseismic activity is a continuous process releasing stress gradually, as, for example, seen in the Renqiu oil field, China [*Genmo et al.*, 1995].

[16] Since the fall of 2002, a seismic seafloor-monitoring four-component array has been operating at Ekofisk using Micro-Electro-Mechanical (MEM) high-resolution sensors. So far, this survey has not revealed any seismic events either from the reservoir or from the overburden, probably due to higher noise levels on the seafloor compared to monitoring from a well.

3. Seismological Far-Field Observations

[17] The 7 May 2001 Ekofisk event was well recorded on seismic stations with an epicentral distance of 318 to 2500 km. Waveform data from more than 150 short-period and broadband stations were collected. The seismograms were dominated by long-period signals and *P* and *S* wave onsets were difficult to read for any station. This is unusual compared to most earthquakes offshore of the Norwegian coast, which show clear body wave arrivals.

3.1. Epicenter Location

[18] The epicenter determination was based on a total of 51 seismic stations with an azimuthal gap of 83° (Figure 4). Event analysis was performed with the SEISAN earthquake analysis software [*Havskov and Ottemöller*, 2001] and the location was determined with the HYPOCENTER program [*Lienert and Havskov*, 1995]. The location program computes travel times based on a one-dimensional velocity model. Two average velocity models were used for comparison (auxiliary material[1], Table A1). The first model is valid for southwestern Norway [*Havskov and Bungum*, 1987], while the second model was derived from the velocity structure determined along the Mona Lisa seismic profile that crosses the Central Graben south of Ekofisk [*Nielsen et al.*, 2000]. The epicenter determined with the first model is at 56.567°N and 3.179°E with an origin time of 0943:33.8 UT [*Atakan et al.*, 2001]. The formal errors (90% confidence) are 4.7 km in latitude and 7.6 km in longitude (Figure 2). The 2 km difference between the two models is insignificant compared to the uncertainties. The epicenter was on the northwestern flank of the Ekofisk field. However, the error ellipse covered about two thirds of the field.

[19] In general, source depth determination requires arrival time data from stations within a focal depth's distance. In this case a hypocentral depth could not be resolved, given the shortest hypocenter-station distance of 318 km. The first arrivals at distances >300 km are critically refracted waves that travel along the Moho interface. Additional phases, such as depth phases that would help to constrain the depth, could not be identified.

3.2. Source Mechanism

[20] Regional broadband waveforms recorded at distances of 350 to 2200 km (Figure 4) were inverted for the seismic moment tensor and to constrain the hypocentral depth. Most stations were located in the southeastern quadrant. The only station toward northwest, on Jan Mayen Island, is distant and the travel path crosses continental and oceanic crust. All other paths are entirely within continental
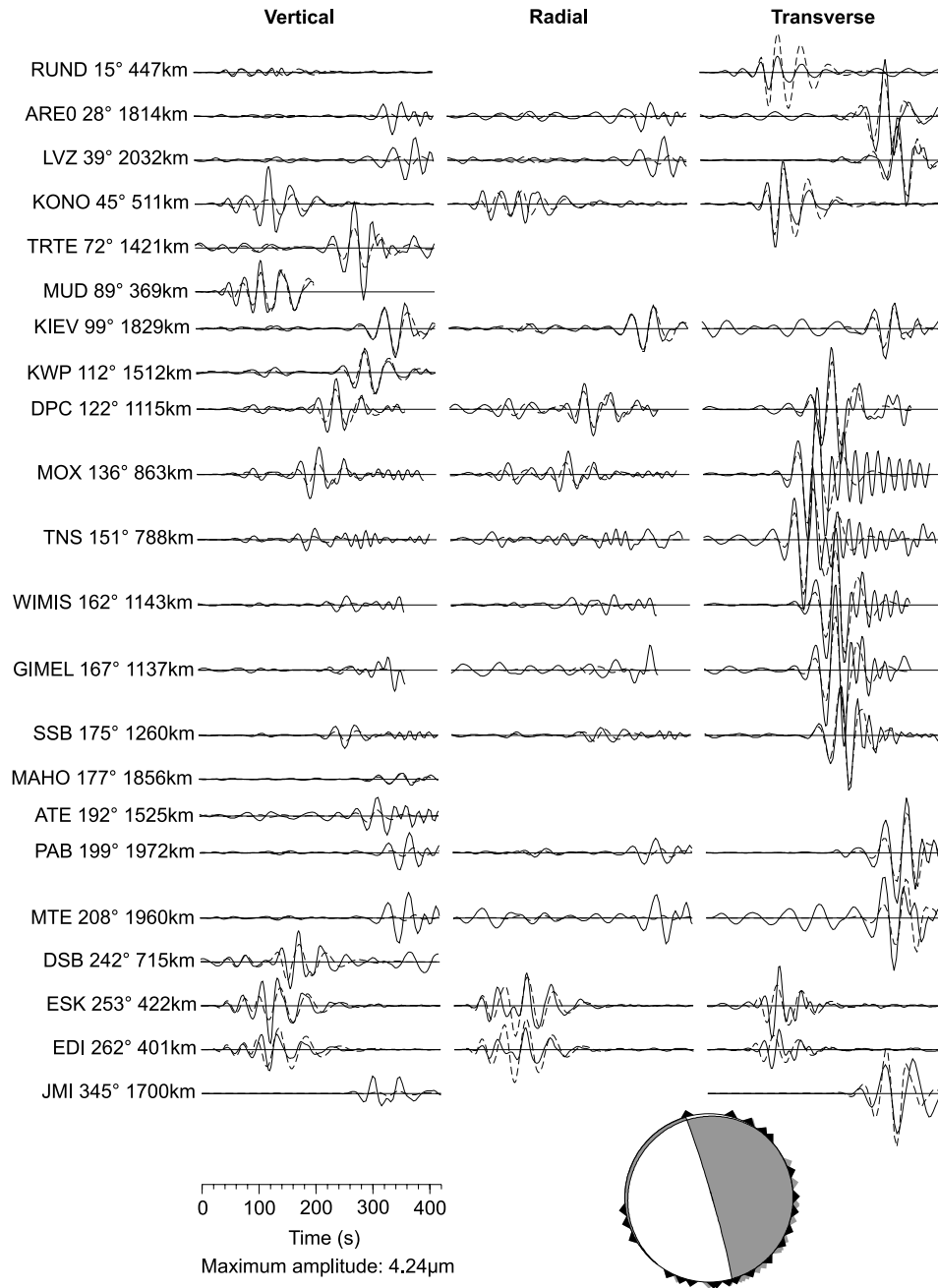
Figure 5. Observed (solid) and synthetic (dashed) seismograms in the 40–60 s passband assuming a 3 km focal depth. Stations are listed in azimuthal order; numbers next to station codes correspond to event-station azimuth and distance. Triangles on the fault plane solution (lower hemisphere projection) depict the coverage (black for stations shown, grey for stations used but not shown). Seismogram amplitudes are normalized assuming cylindrical geometric spreading.

crust. We selected stations to cover all directions as evenly as possible.

[21] The method inverts all three-component waveforms simultaneously by minimizing the least squares misfit between observed and synthetic seismograms. We used three-component data whenever possible and discarded noisy traces. Earthquake depth is found by grid search over trial depths. From 2 to 7 km depth the increment is 1 km, and below depths of 9 km, it is 3 km. For details, refer to *Nabelek and Xia* [1995]; for applications to European earthquakes, refer to *Braunmiller et al.*

[2002]. Synthetic seismograms were calculated for simple 1-D velocity structures using a frequency–wave number technique [*Bouchon*, 1982]. We tried several structures (auxiliary material, Figure A1) [*Braunmiller et al.*, 1994; *Nielsen et al.*, 2000] to investigate model influence on the source parameter estimates. We modeled the data at long periods to avoid signal ringing caused by the thickly sedimented travel paths through the North Sea.

[22] Figure 5 shows the waveform fit in the 40–60 s passband for our preferred crustal model (thick solid line in auxiliary material, Figure A1). A pure shear dislocation
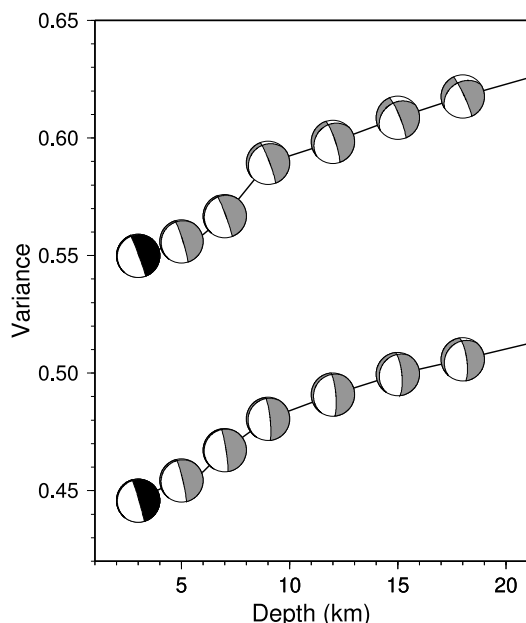
Figure 6. Misfit versus hypocenter depth plot. Bottom curve shows misfit inverting stations up to 2200 km distance in the 40−60 s passband. Top curve shows the misfit inverting only stations up to 1200 km distance in the 30−50 s passband. Black marks the best fit depth. The shallow minima are pronounced. The fault plane solutions are stable over a wide depth range.

source (faulting) explains the data. The two nodal planes correspond to a near-vertical, mostly normal, dip-slip mechanism striking NNE (strike, dip, rake of 344, 87, −94°) and an oblique-normal slip along a near-horizontal plane striking ENE (strike, dip, rake of 217, 5, −37°), respectively. The azimuthal station distribution constrains the mechanism well. The shallow source depth and moment tensor solution appear well resolved (Figure 6). Using a 5% variance increase as cutoff places the source in the upper 7 km of the crust.

[23] Varying station distributions and passbands invariably resulted in very shallow source depths and a similar mechanism with NNW trending N axis. To achieve the best possible azimuthal coverage, data were modeled up to 2200 km in the 40−60 s passbands. The average event-station distance was 1200 km. To reduce the effect of the crustal model, the analysis was limited to stations less than 1200 km from the epicenter (average distance 800 km). The best depth and mechanism in the 30−50 s passband are not affected by this change (Figure 6, top curve).

[24] The same analyses were performed for the other velocity models. Size estimates, the mechanism for shallow depths and its orientation all remained largely unaffected. Only source depth estimates differed. Shallow depths were obtained for the standard model used by the Swiss Seismological Service [*Braunmiller et al.*, 2002] (between 3 and 6 km) with well-developed misfit minima. Best depths for the layer over half-space model are near 10 km and vary for preliminary reference Earth model (PREM) synthetics from 9 to 24 km depending on passband and stations used. Overall misfits are about 20% higher for these latter two,

probably less realistic, models. Their misfit curves also do not vary much with depth resulting in effectively unresolved depth estimates. We favor a very shallow source depth but recognize that source depth estimates are sensitive to the crustal model.

[25] The seismic moment estimates depend on the velocity structure. For waveform modeling, crustal models were chosen to provide approximate phase matches at regional distances. However, true velocities in the Ekofisk overburden ($v_s \approx 1$ km/s and Poisson ratio ∼0.33 [*Nagel*, 1998]) are significantly lower than for any of the models. Higher velocities in the source region map directly onto higher seismic moment. Replacing the uppermost 4 km crust of our preferred model with the Ekofisk overburden values provides a seismic moment of about $M_0 = 5 \times 10^{15}$ N m. Uncertainties in source depth, propagation path, and receiver effects translate easily into a M_0 uncertainty factor of 2.

3.3. Source Spectrum

[26] To investigate whether the spectra of the 2001 event were anomalous, the source spectra were compared to the 31 March 1988 and 18 August 2000 events as these were located in the vicinity of Ekofisk. For comparison, both P and S wave spectra at station Eskdalemuir (ESK) were computed for the three events (Figures 7a and 7b). The P wave spectra confirm that the 2001 event was the largest followed by the 2000 event. The S wave spectra show a similar picture. However, above about 3 Hz the spectral levels are very similar between the three events, and it appears that the 1988 event has more high-frequency energy.

[27] For comparison with theoretical spectra assuming the ω^2 model [*Brune*, 1970] we computed displacement spectra corrected for attenuation using the method of *Ottemöller and Havskov* [2003] (Figure 7c). The shape and long-period level of the spectrum is given by the corner frequency and the seismic moment; both can be derived from the observed source spectrum. The correction applied for attenuation is given by $\exp(-\pi f\, t/Q(f))\, \exp(-\pi f\kappa)$, where t is the travel time, $Q(f)$ the frequency-dependent quality factor and κ accounts for near-surface losses [*Singh et al.*, 1982]. Applying the standard Q correction for Norway given by $Q(f) = 440\, f^{0.7}$ [*Kvamme et al.*, 1995] and $\kappa = 0.02$ (model 1) resulted in a rather low corner frequency of $f_c = 0.1$ Hz, implying a lack of energy excited at higher frequencies and a longer rupture duration. However, this apparent lack of high-frequency energy could be caused by high attenuation, where sediment thickness reaches about 10 km. Therefore a second model combining $\kappa = 0.1$ for the near-source region, equivalent to 5 s travel time at $Q = 50$, and $Q(f) = 150\, f^{0.7}$ for the remaining travel path appears more appropriate in the absence of a well defined Q model for the North Sea (Figure 7d). The observed source spectrum based on the second Q model was matched with a theoretical ω^2 model assuming a stress drop of 3.8 bars and a seismic moment of 1.5×10^{15} N m (Figure 7c). A range of values for the source radius, stress drop and slip were computed to reflect the uncertainties involved (Table 1).

[28] Comparing the observed spectra for the two Q models demonstrates the nonuniqueness involved in attempting to
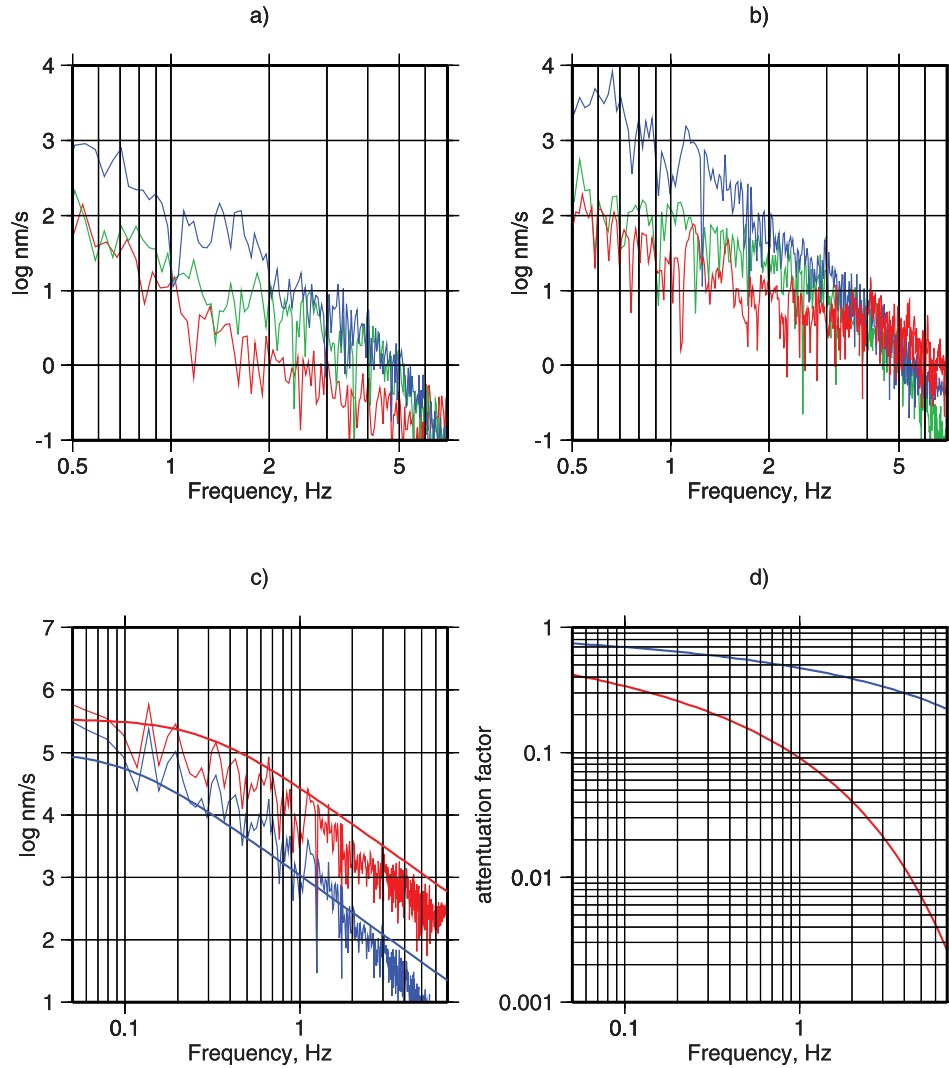
Figure 7. (a) Displacement spectra for station ESK computed from 25 s P wave signal for the 31 March 1988 (red), 18 August 2000 (green), and 7 May 2001 (blue) events. The spectra are not corrected for attenuation. (b) Same as Figure 7a but for S wave signal. (c) S wave displacement spectrum for the 7 May 2001 event corrected for two attenuation models, $Q_1(f) = 440f^{0.7}$ and $\kappa_1 = 0.02$ (blue) and $Q_2(f) = 150f^{0.7}$ and $\kappa_2 = 0.1$ (red). The synthetic spectra are for $\Delta\sigma = 3.8$ bars, $Mo = 1.5 \times 10^{15}$ N m, $Q_1(f)$ and κ_1 (red) and $\Delta\sigma = 0.05$ bars, $Mo = 4.7 \times 10^{14}$ N m, $Q_2(f)$ and κ_2. The synthetic spectra illustrate the uncertainties and represent a range of solutions. d) Attenuation factor for the two models $Q_1(f)$ and $\kappa1$ (blue) and $Q_2(f)$ and $\kappa2$ (red).

determine spectral parameters. While Q model 1 indicates a low stress drop, Q model 2 explains the lack of higher-frequency energy observed at distances of more than 300 km through high near-source attenuation. The nonuniqueness could be resolved with near-field data, which do not exist for the 2001 event. The apparent lack of high frequency energy is also seen when comparing the event size using various magnitude scales as described next.

3.4. Event Size

[29] The event size has important implications for evaluating the response of the infrastructure at Ekofisk from an engineering point of view. The seismic moment determined from the moment tensor inversion, assuming low near-surface shear wave velocities, was $M_0 = 5 \times 10^{15}$ N m, whereas a value of $M_0 = 1.5 \times 10^{15}$ N m was determined

Table 1. Range of Source Parameters for Extreme Values of Corner Frequency f_c and Seismic Moment M_0[a]

Parameter	Low Seismic Moment	High Seismic Moment
M_0, N m	4.7×10^{14}	1.5×10^{15}
f_c, Hz	0.1	0.3
R, km	3.5	1.2
σ, bars	0.05	3.8
d, cm	6	47

[a]Source parameters were determined from observed displacement source spectra (Figure 7). The derived parameters are the source radius ($R = 0.35\, v_s/f_c$) for a circular fault, the stress drop ($\sigma = 0.44\, M_0/R^3$) and the seismic slip ($d = M_0/(\mu\pi R^2)$). The following parameters representative of the overburden at a depth of about 6000 feet (1829 m) were used [Nagel, 1998]: S wave velocity $v_s = 1$ km/s, density $\rho = 2.2$ g/cm^3, and shear modulus $\mu = 1$ GPa.
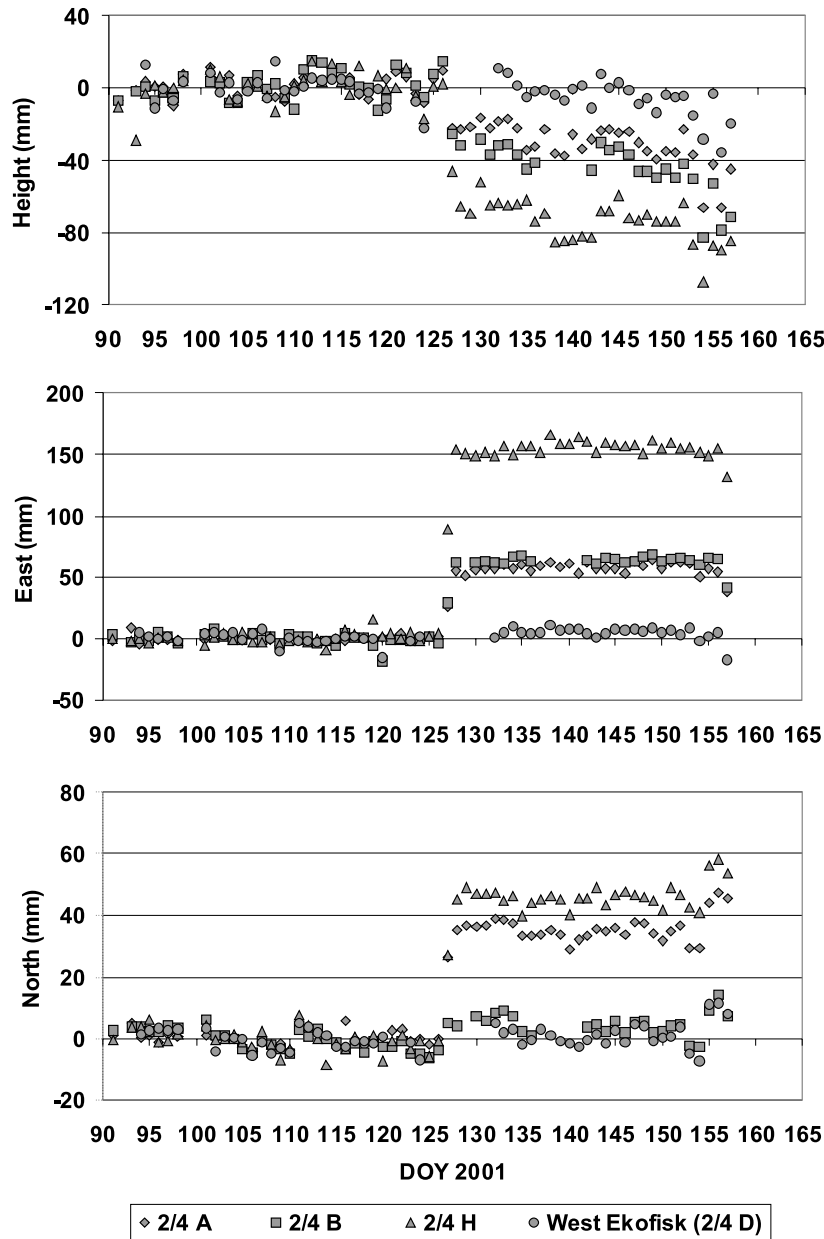
Figure 8. Long-term GPS data as recorded on platforms in the Ekofisk field. Permanent changes are seen in the GPS data from platforms 2/4-A, 2/4-B and 2/4-H, which are all located in the central part of the Ekofisk field (by courtesy of Statens Kartverk, Norway).

from the long-period part of the displacement spectrum, assuming high near-source attenuation. The corresponding moment magnitude [*Kanamori*, 1977] values are $M_w = 4.4$ and $M_w = 4.1$, respectively. In addition, three amplitude-based magnitudes were computed. These were the body wave (m_b) measured on *P* waves [*Veith and Clawson*, 1972], the surface wave (M_s) [*Karnik et al.*, 1962], and the local magnitude (M_L) derived for Norway [*Alsaker et al.*, 1991] measured on *Lg* waves. The results computed as averages from several stations were $m_b = 4.4$, $M_s = 4.6$ and $M_L = 3.0$. While m_b and M_s are similar to M_w, the M_L value is significantly lower. Compared to the other scales M_L is measured at higher frequencies, and the low value of M_L is due to low excitation at frequencies above 1 Hz. The difference between M_L and m_b, which is measured at

$\sim$1 Hz, could be explained by measuring amplitudes of different wave types as well as frequency.

4. Near-Field Observations

4.1. GPS, Interplatform Distance, and Tide Gauge Measurements

[30] Global Positioning System (GPS) monitoring at Ekofisk started in 1985 and is used to monitor gradual subsidence. Since autumn 2000, continuous GPS data were acquired on the Ekofisk 2/4-H, 2/4-A and 2/4-B platforms (as well as six other locations in the area) using Ashtech FX-CORS dual-frequency receivers. The GPS antennas are mounted on a mast about 200 m above the deck of the platforms. The GPS data normally show the gradual and
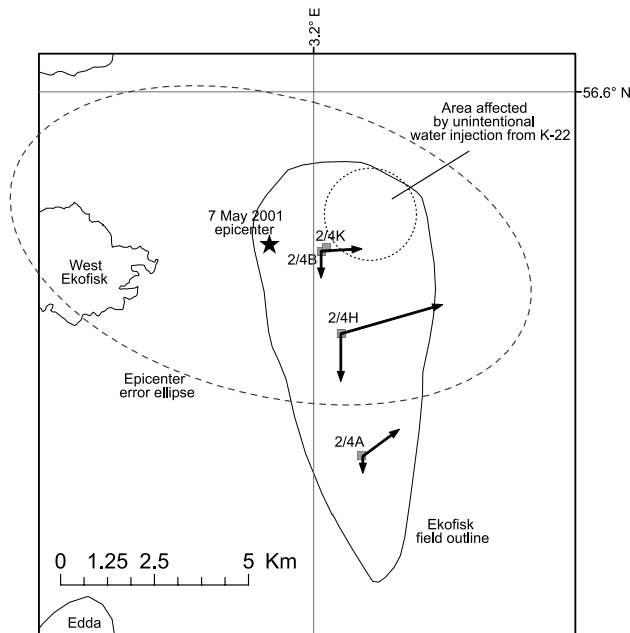
Figure 9. Horizontal and vertical (in direction of decreasing latitude) GPS data displacement vectors for 7 May 2001. The horizontal vector for the 2/4-H platform corresponds to 16 cm; scaling is the same for vertical direction.

continuous changes due to subsidence. Comparison of GPS data from before and after the 7 May event showed several centimeters of static displacement of the antenna on the three platforms in both vertical and horizontal directions (Figures 8 and 9). The largest displacement was recorded on the centrally positioned Ekofisk 2/4-H platform, while 2/4-A and 2/4-B showed less displacement. The apparent horizontal movement may have been due to a combination of horizontal displacement and localized tilt. A small change in tilt would explain large horizontal movements of the antennas. No displacement was observed from GPS data recorded on the Eldfisk and West Ekofisk platforms.

[31] Interplatform distance measurements (resolution of 5 mm) immediately after the event did not show any significant changes compared to previous measurements. The change in distance between platforms derived from the GPS data was about 15 mm and thus smaller than the actual displacement due to the direction of movement and the geometry of the platforms. It is possible that the change in distance was not detectable with the interplatform distance measurements, although the estimated resolution suggested otherwise.

[32] Water height was measured at the southern and northern flare bridges, at a distance of about 800 m to the south and north from the 2/4-H platform, respectively, through laser tide gauge instruments. These tide gauge data show large variability and are not routinely analyzed. Specific investigation of the data showed 8 cm permanent downshift of the flare relative to the sea surface after the time of the seismic event (the clock of the tide gauge sensor was not accurately calibrated). The 8 cm vertical drop compared to water height is consistent with the reported

vertical drop estimated from the GPS data at the 2/4-H platform.

4.2. High-Resolution Bathymetric Survey

[33] The seismic data and GPS observations indicated a shallow depth for the seismic event. To investigate whether the event reached the surface or caused slumping, ConocoPhillips carried out a high-resolution (resolution lateral 10 m, vertical ±20 cm) bathymetric survey over the Ekofisk, West Ekofisk, and Eldfisk fields (Figure 2) 2 months after 7 May 2001. The most recent previous survey in the same area was acquired during the summer of 1999. A differential bathymetric map was computed to compare the 1999 and 2001 surveys (Figure 10). The map displays subsidence greater than 40 cm in the southern parts of the Ekofisk field, mapping the expected N-S elongated subsidence bowl. In contrast, the northern part of the field has risen between 1999 and 2001 by about 25 cm. Only minor subsidence was expected in this part of the field due to low extraction rates. However, uplift would not be expected under normal conditions.

[34] Detailed wavelength filtering and Landmark Sobel edge detection was performed on the 2001 data. The resulting image with a vertical resolution of <10 cm did not show any features apart from the pipelines. This result ruled out any slumping or breaking of the sea bottom with dimensions greater than the vertical resolution.

4.3. Pressure Gauge Records and Reservoir Compaction Monitoring

[35] Ten wells had downhole pressure and temperature gauges working on the Ekofisk field on 7 May 2001. The gauge data were checked for differences during the event. All wells, except 2/4-X-09 (Figure 10), were on production and did not show any changes related to the event. Close inspection of the 2/4-X-09 well that is shut in (nonproducing), showed a small pressure increase of $\sim$3 psi (20.7 kPa) at 0945 UT on 7 May [*Nielsen*, 2003]. This pressure increase may be the result of the seismic event causing vibration of the gas-oil-water column such that gas liberation took place. The pressure is very sensitive to changes in the fluid composition, and may easily account for the observed pressure increase [*Nielsen*, 2003]. Alternatively, a change in the gauge depth relative to the nearest reservoir perforations may contribute to the pressure increase. A pressure increase can be simulated as a change in the hydrostatic pressure caused by a pure distance change between the gauge and the nearest reservoir perforation. A 3 psi increase in pressure would reflect 7 feet (2.1 m) compaction in the reservoir [*Nielsen*, 2003]. Compaction of this size between the gauge and the reservoir does not match the well condition after 7 May, which remained intact. However, it is possible that small-scale compaction has contributed to the increase in pressure.

[36] Several wells in the Ekofisk field were completed with radioactive markers to routinely measure the reservoir compaction rates [*Nagel*, 1998]. Abrupt changes in the distance between these radioactive bullets, seen in Compaction Monitoring Instrument (CMI) logs, would indicate a deviation from normal reservoir compaction behavior. Compaction rates at the wells 2/4-X-12 and 2/4-C-11A were as expected and do not explain the pressure change
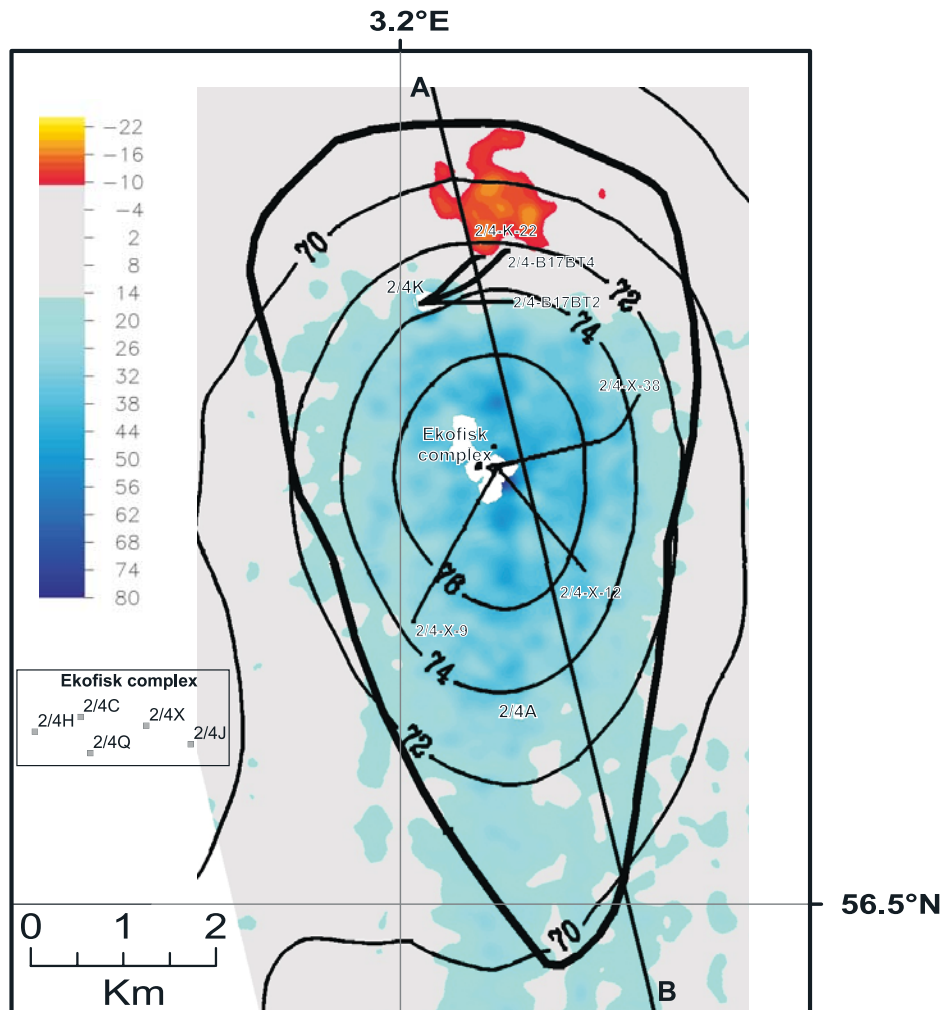
Figure 10. Differential bathymetry between the 1999 and 2001 detailed bathymetry surveys. The map scale is in centimeters. A sea bottom uplift is seen on the northern flank of the field (red). Total subsidence data up to 2001 are shown in decimeters by contour lines. The central parts of the field exhibit the normal subsidence features (blue). The surface projections of wells are indicated by black lines. The line crossing the field in NNW-SSE direction gives the location of the section shown in Figure 3. Locations of platforms in the Ekofisk complex are plotted on the inset map at a different scale.

at 2/4-X-09 (auxiliary material, Figure A2). The CMI logs are also done for the overburden where they normally show no compaction. The expected change on 7 May was below the resolution and therefore not detected.

4.4. Hydrocarbon Extraction and Water Injection

[37] It might be expected that an earthquake of significant size would impact production performance due to well failures. ConocoPhillips therefore closely monitored the production well performance after the event to capture specific areas in the field with abnormal production behavior. However, the Ekofisk production performance has not shown any unpredicted behavior.

[38] During 2002, while drilling from the northern 2/4-B platform at two locations (2/4-B17BT4 and 2/4-B17BT2, Figure 10) in the northern flank of the field, abnormally high pressures were observed in the overburden (6000–7000 feet (1830–2130 m) true vertical depth subsea (TVD SS)). This led to reinvestigation of the injectors in that area

and well intervention was performed in several wells to resolve problems. It was found that some of these wells had developed casing deformations. Closer investigation confirmed that due to a previous reservoir collapse one water injector (2/4-K-22, Figure 10) was injecting 15,000 barrels/d (2385 m³/d) cold water into the overburden at a depth of 6000–7000 feet TVD SS (1830–2130 m). Minor changes in injectivity, observed in 1999, were now considered to be related to the start of injection into the overburden. A total of 12×10^6 barrels (1.9×10^6 m³) of cold water may have been injected before the seismic event happened. Since the 2001 event, several wells in the northern part of the field around 2/4-K-22 have developed restrictions at a depth of ~4500 feet (1372 m). This is shallower than generally seen for well failure prior to the 2001 event.

[39] The overburden injection was considered to be the cause of the abnormal overburden pressure in its vicinity. The location of 2/4-K-22 coincides with the uplift in the northern part of the field seen in the differential bathymetry
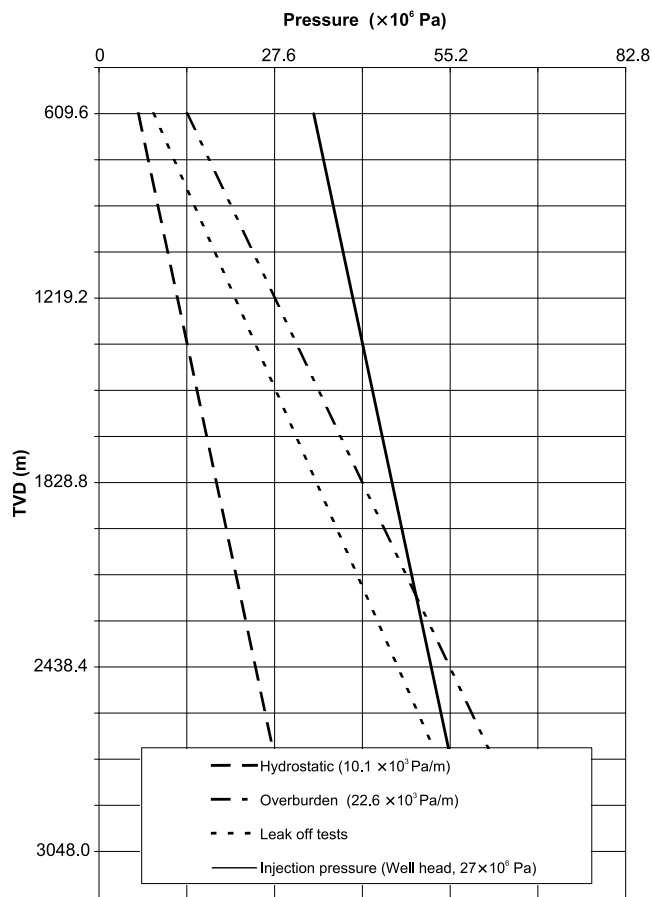
Figure 11. Pressure gradients for the Ekofisk overburden and injection pressure at K22. The Ekofisk overburden gradient is less than the 22.6×10^3 Pa/m overburden pressure and closer to 20.4×10^3 Pa/m caused by overpressure/undercompaction. The Ekofisk overburden is overpressured from 3000 feet (914.4 m) to the top of the reservoir. The injection pressure is the combined result of the pressure at the wellhead and the weight of the injection column. Injection pressure is above leak-off test (LOT) pressure at all overburden levels and from 7500 feet (2286 m) upward above 22.6×10^3 Pa/m lithostatic pressure.

data (Figure 10). The same area was also identified as showing areal time differences in the overburden section between seismic surveys in 1999 and 2003, which were caused by the overpressure. ConocoPhillips monitors annulus pressures daily on both production and injection wells to ensure that production and injectors are not in communication with nonreservoir formations. The unintentional water injection into the overburden from 2/4-K-22 was at first not recognized as deviation in the annulus pressures, because the well had a permanent cement block in the lower parts of the tubing annulus and the leak most likely occurred below this cement plug. The cement plug was considered low risk as it was expected that reservoir collapse and leakage into the overburden would be noticed from the injection rate and pressure monitoring. Water injection in the leaking well was closed down permanently in 2002.

[40] Figure 11 demonstrates that the water injection pressure was above the minimum horizontal stress derived from leak-off test (LOT) data throughout the entire overburden, down to the top of the reservoir. The water injection pressure was thus above fracture pressure in the entire overburden consequently leading to fracture of the shale and mud rocks and opening void space for water circulation. From the size of the area that was uplifted (Figure 10) it was concluded that crack propagation was generally horizontal. However, the migrating injected water possibly also followed minor vertical faults. The injection pressure was sufficient to overcome the overburden weight from about 7000 feet (2133 m) upward and had the ability to lift the entire overburden.

[41] We also concluded that drill cuttings injection did not contribute to the uplift (auxiliary material, text 1).

4.5. Macroseismic Observations and the Platform Structure Assessment

[42] The ground shaking caused by the 7 May event was felt by people working on the Ekofisk platforms. A macroseismic survey was conducted based on the European Macroseismic Scale (EMS) [Grünthal, 1998; Atakan et al., 2001]. Questionnaires were sent to all platforms that were occupied by people at the time of the earthquake. In addition to the Ekofisk platforms, information was collected from the neighboring platforms. 33 out of 36 returned questionnaires contained sufficient information for evaluation (auxiliary material, Table A2). The event was felt strongly in the central and northern sections of the Ekofisk field. No information was available from the southern platforms (e.g., 2/4-A, an unmanned platform). The maximum intensities may have reached as high as VII, but in general intensity VI is consistent throughout the Ekofisk field. In the Eldfisk and Embla fields in the south the event was felt only weakly. Maximum intensities were lower in the Tor field about 20 km northeast of Ekofisk (Figure 2). It seems likely that the response of the platform structures played an important role in the way people felt the event. Description of "swinging" was dominant on the platforms that either have a large mass or are away from the central structures (examples are 2/4-K and 2/4-H). Descriptions such as "felt like a collision of a supply boat" were dominant in the central parts of the field (examples are 2/4-Q, 2/4-C, 2/4-X). In a few cases, the description "difficult to stand up" was used which may indicate higher intensities (i.e., VII) and also support "swinging" description (examples are 2/4-C, 2/4-K).

[43] On the basis of the above data and the consistency of results showing maximum intensities of VI in the entire Ekofisk field, a positive correlation between the computed epicenter and the highest intensities was established. The fact that the event was strongly felt only at structures in the central part of the Ekofisk field, and more weakly with increasing distance, suggests a shallow source depth.

[44] Detailed mechanical integrity modeling was undertaken to investigate the effect of the seismic event on the platform structures. Because of the lack of knowledge of acceleration levels in the near field, several worst case scenarios were modeled. The modeling revealed potentially overstressed parts of the platforms. These parts were then closely inspected for failure and fatigueness. How-

ever, no sign of damage to the platform structures was found.

5. Discussion

5.1. Unintentional Water Injection

[45] The differential bathymetry map (Figure 10) showed that the northern flank of the Ekofisk field had been significantly uplifted instead of the expected slight subsidence. Drilling into the overburden revealed unexpectedly high pressures in the uplifted area. These high pressures were also seen as time differences between seismic surveys in 1999 and 2003. The source of the unusual high pressures was a water injector that unintentionally leaked into the overburden. The depth (6000–7000 feet (1828–2134 m) TVD SS) and location (northeastern flank) of the leakage and observed overpressure coincided, suggesting that the uplift was explained by the overburden being hydraulically jacked up. Fracture modeling for the overburden showed that horizontal fracture growth would be inhibited [*Nagel and Strachan*, 1998]. However, from the observations of overpressure at depth over a substantial area, we conclude that horizontal fracturing subsequently followed by uplift of the overburden had indeed occurred. Possibly, cold water injection into the very shaley undercompacted and already overpressured overburden with horizontal layering temporarily created local sealing capacities and stress conditions, such that the water, which was continuously injected at a high rate, was trapped under pressures exceeding the overburden weight.

5.2. Hypocenter Location, Source Dimension, and Event Size

[46] The epicenter of the 7 May 2001 seismic event, was located within the outline of the Ekofisk field. This result, initially derived from seismic far-field data, was confirmed by macroseismic data and GPS observations from platforms in the Ekofisk field. Comparing GPS data from before and after 7 May revealed that vertical subsidence of up to 8 cm had taken place. Horizontal displacement of up to 15 cm observed with GPS data was not confirmed by interplatform distance measurements, probably because the change in distance between platforms was too small to be resolved. The vertical movement seen on the platforms may be due to compaction either in the overburden (depth <3000 m) or the reservoir (depth >3000 m). However, pressure gauge and reservoir compaction data, production performance and the lack of well failure showed that compaction associated with the 7 May event did not occur within the reservoir. Rather, the source was confined to the overburden. The overburden has very low shear strength (μ < 1 GPa), which, prior to the 7 May event, resulted in small-scale horizontal slip as observed from well failure. The hypothesis of a shallow depth for the 7 May 2001 event is supported by results from the moment tensor inversion. The macroseismic observations also agree with a shallow depth, since a deeper event would have been felt on platforms at greater distances.

[47] The event dimensions were estimated through spectral analysis. The seismic observations at large distances (>300 km) show a lack of high frequency signal, which was probably attributed to a low stress drop, slow rupture process and high near-source attenuation. The source radius estimated from the corner frequency was in the range 1.2–3.5 km (Table 1) and gives a maximum source area of 38.5 km^2, which is almost the size of the Ekofisk field. The location error ellipse (Figure 9) covers more than the northern half of the field and considering its dimensions, the source would fit into the northern part including the area affected by water leakage. Translating seismic moment and source radius into fault slip gave values of 6 to 47 cm ($M_0 = \mu$ Ad, where μ = 1 GPa is shear modulus, A is fault area and d is fault slip). The fact that the dense network of wells was not noticeably affected by the seismic event indicates that movement did not exceed ~10 cm. To explain the observed seismic moment then requires the larger estimated source radius ($R \approx 3.5$ km).

[48] The upper limit for stress drop was estimated as σ = 3.8 bars, while the lower limit was given by σ = 0.05 bars. Uncertainties in stress drop are large, but either way, the stress drop was significantly below the interplate average of 30 bars [*Kanamori*, 1975]. The moment magnitude scale is based on the relation between energy and seismic moment for a constant stress drop (30 bars), while in fact energy is proportional to the product of stress drop and seismic moment [*Kostrov*, 1974] and thus dependent on stress drop. The 7 May event (M_w = 4.1–4.4) therefore did not release as much energy as a typical stress drop event of that size. The model of a low stress drop event is supported by the inspection of platform structures that did not reveal any sign of damage, possibly due to the lack of high frequency energy. The interpretation as shallow low stress drop event is similar to the Wilmington subsidence earthquakes [*Kovach*, 1974]. There, slip occurred on near-horizontal planes above the reservoir. The Willmington events, similar to the Ekofisk event, while generating emergent body wave, excited surface waves strongly.

5.3. Model of the Source Processes

[49] The exact nature of what happened before and during the seismic event on the northern flank remained unresolved, since bathymetry and pressure measurements are available only for 1999 and the period after 7 May. However, it is likely that the seismic event would not have occurred without unintentional water leakage, because shear strength in the overburden is low and no previous sizable seismic event associated with overburden compaction has been observed. The overburden stress pattern was altered by water injection, but we expect that the stress changes due to reservoir compaction are of importance in understanding the source mechanism. The expected horizontal stress pattern in the overburden (Figure 12) due to reservoir compaction is compression in the center of the subsidence bowl and tension on the flanks [*Segall*, 1989]. The high pore pressure, caused by water injection into the overburden, reduced the effective normal stress and according to the Coulomb failure criterion [e.g., *Scholz*, 2002] facilitated movement due to horizontal shear stresses, which are concentrated over the edge of the reservoir [*Nagel*, 1998]. Additionally, the overpressured zone was weakened horizontally. It therefore seems likely that slip initiated in the overpressured area on the northern flank above a depth of about 7000 feet (2134 m) TVD SS. Uplift and overpressure were observed after 7 May 2001, and thus changes during the seismic
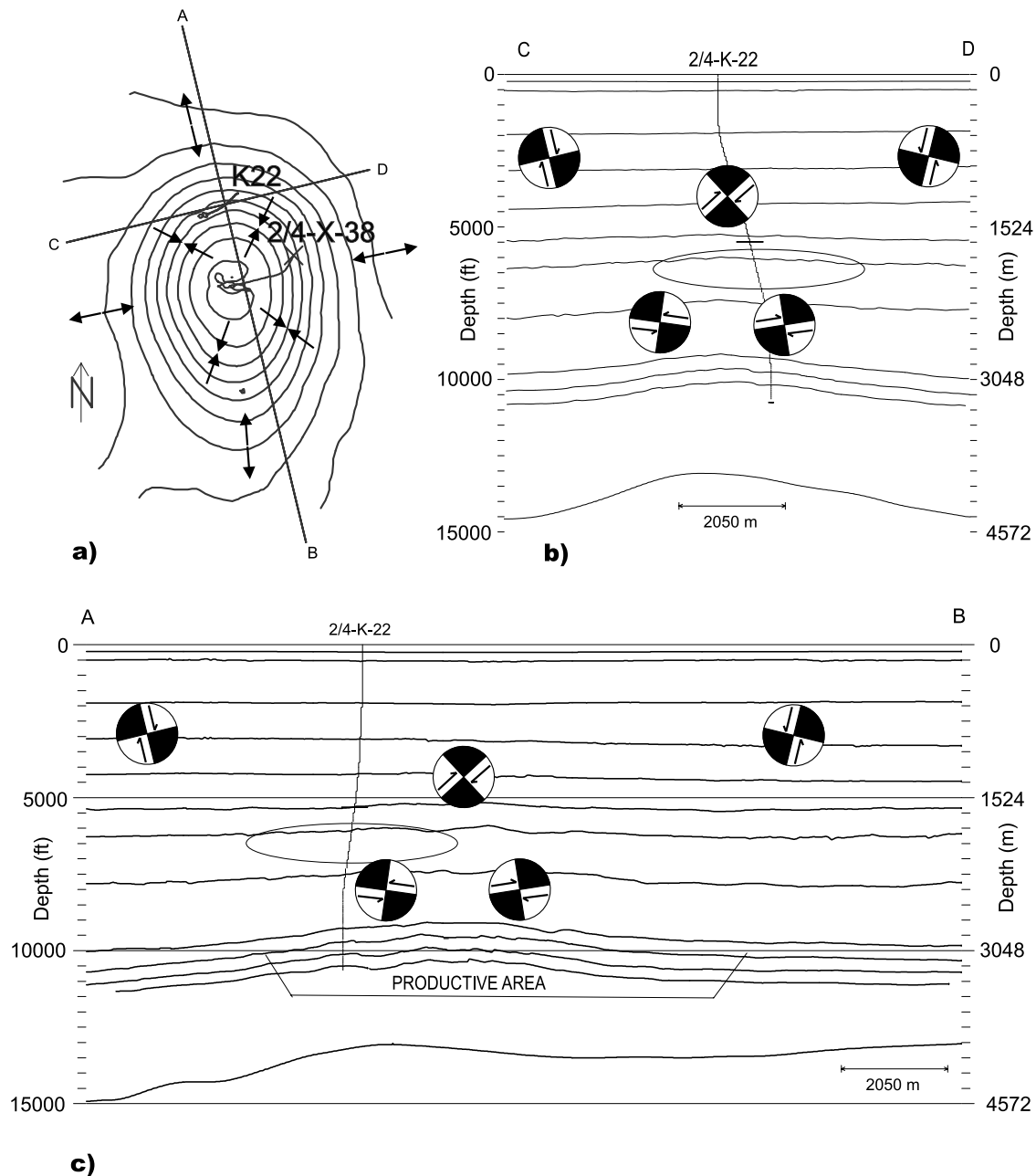
Figure 12. Schematic overview of stress distribution and expected movement in the overburden due to reservoir compaction, not taking into account unintentional water injection (following *Segall* [1989]) (Figure 6). In Figure 12a, arrows show expected stress pattern, compression near the center of the subsidence bowl, and extension on the flanks. Contour lines represent subsidence; straight lines give location of sections given in Figures 12b and 12c, which are taken across the area affected by unintentional water leakage from 2/4-K-22 (well path shown) indicated by the ellipse at depth of about 6000–7000 feet. Expected orientation of slip planes and direction of shear motion along overburden cross sections are indicated by beach balls, which is normal on the flanks and reverse in the center, respectively [*Segall*, 1989]. The vertical scale is exaggerated by a factor of ~2.

event were not resolved. It is also unclear if and why small-scale slippage was inhibited before the event. Permanent displacement seen on the platforms 2/4-A, 2/4-B and 2/4-H from GPS data required that larger parts of, or even the entire, Ekofisk overburden were involved, unless they were explained in terms of elastic deformation. The overburden may have flexured coseismically into the subsidence bowl involving both horizontal and vertical motion, leading to the displacement seen on the platforms. This setting of the overburden was triggered by failure of the overpressured area. Future stress modeling would help to quantify the problem. However, detailed knowledge of physical properties in the overburden, beyond what is known at present, would be required.

[50] The seismic signal in the far field is the superposition of movement that may have occurred on several slippage planes; the moment tensor solution reveals the dominant slip orientation and direction. The two nodal planes from the moment tensor inversion are near horizontal and near vertical. Even considering the lower estimate for source radius of ∼1 km, it seems difficult to fit the source onto a single near-vertical plane in the overburden without reaching the surface or the reservoir. More likely, the source radius was larger, which practically rules out a single near-vertical fault plane. This leaves the predominantly near-horizontal solution, which is possible as seen from near-horizontal casing failure, combined with small-scale vertical movement. Horizontal slippage was facilitated by increased pore pressure due to water injection into clay-rich shales. Even the larger source radius ($R = 3.5$ km) can easily be accommodated within the overburden if it is oriented horizontally. The moment tensor solution showed normal slip of the northwest dipping near-horizontal plane, which agrees with the expected sense of motion on the northwestern flank (Figure 12). The near-horizontal plane would also match the setting of the overburden on the northeastern flank. However, this solution, with the hanging wall moving W-NW, is not supported by the GPS data, indicating platform movement to the east. Normal movement on the near-vertical plane in the northwestern area would agree with both GPS data and the moment tensor solution. Alternatively, the GPS data may reflect flexure of the overburden into the subsidence bowl, with displacement down and to the center of the field. Direction of displacement of the platforms in the center of the field would have been different from the northeastern flank. Because of the apparent mismatch of the moment tensor solution and GPS measurements, it is not clear where in the overburden the dominant seismic energy release occurred.

[51] One of the key objectives of this work was to investigate whether the event was induced. Knowledge of the source location and source process of the setting within the overburden implies that the event was induced. Without unintentional water injection into the overburden at the northern flank, the event most likely would not have occurred as seen by the preceding 30 years of aseismic subsidence. Pressures remained high and the overburden uplifted after the 7 May event, but since the central overburden has been compacted and the unintentional water injection has stopped, it appears unlikely that a similar event would occur in the near future.

[52] An important outcome from this study is that earthquakes with $M_w > 4$ can occur at shallow depth within poorly consolidated and overpressured mud and shale rocks. Generally, such rocks are considered to be weak and to deform aseismically. The results from this work suggest that some of the strain in weak shallow rocks can be seismogenic.

6. Conclusion

[53] The combination of near- and far-field observations allowed us to develop a model for the processes leading to the 7 May 2001 seismic event at Ekofisk. Far-field seismic data suggested that the event occurred near the Ekofisk field at shallow depth. Fully resolved hypocenter param-

eters, however, would require near-field data, which were not available. Such near-field data will be of importance to accurately locate any future similar seismic event elsewhere. Our main results are as follows:

[54] 1. The event occurred within the outline of the Ekofisk field as shown by GPS measurements and macroseismic observations on the platforms and the hypocenter location.

[55] 2. The source was confined to the overburden, since sudden compaction seen as seafloor subsidence in the GPS data did not occur within the reservoir as ruled out by compaction log data.

[56] 3. Slip, most likely on a near-horizontal plane, was facilitated by increased pore pressure in the overburden on the northern flank due to unintentional water injection, which led to the overburden being jacked up. However, slip may have taken place on a near-vertical plane.

[57] 4. The event probably initiated on the northern flank and spread to the rest of the field leading to flexure of the overburden into the subsidence bowl. In the center of the field, up to 8 cm vertical subsidence were observed from both GPS and tide gauge measurements.

[58] 5. Because of the location in the overburden and the event's relation to unintentional water injection on the northern flank, we conclude that the event was induced.

[59] 6. The source radius of the event was on the order of $1-4$ km with $M_w = 4.1-4.4$. The event was strongly felt on the platforms. However, it did not cause any damage to structures in the Ekofisk field. The apparent lack of high-frequency seismic energy in the far field was caused by the combination of low stress drop and high attenuation in the source region. The energy released by the source at high frequencies remains uncertain.

References

Alsaker, A., R. Kvamme, R. A. Hansen, A. Dahle, and H. Bungum (1991), The M_L scale in Norway, *Bull. Seismol. Soc. Am.*, *81*, 379–398.

Atakan, K., L. Ottemöller, S. L. Jensen, J. Braunmiller, and A. Ojeda (2001), The Ekofisk seismic event of May 7th, 2001, technical report, Inst. of Solid Earth Phys., Univ. of Bergen, Bergen, Norway.

Bouchon, M. (1982), The complete synthesis of seismic crustal phases at regional distances, *J. Geophys. Res.*, *87*, 1735–1741.

Braunmiller, J., T. Dahm, and K.-P. Bonjer (1994), Source mechanism of the 1992 Roermond earthquake from surface-wave inversion of regional data, *Geophys. J. Int.*, *116*, 663–672.

Braunmiller, J., U. Kradolfer, M. Baer, and D. Giardini (2002), Regional moment tensor determination in the European-Mediterranean area—Initial results, *Tectonophysics*, *356*, 5–22.

Brune, J. N. (1970), Tectonic stress and the spectra of seismic shear waves from earthquakes, *J. Geophys. Res.*, *75*, 4997–5009.

Bungum, H., A. Alsaker, L. B. Kvamme, and R. A. Hansen (1991), Seismicity and seismotectonics of Norway and nearby continental shelf areas, *J. Geophys. Res.*, *96*, 2249–2265.

Chin, L. Y., and N. B. Nagel (2004), Modeling of subsidence and reservoir compaction under waterflood operation, *Int. J. Geomech.*, *4*, 28–34.

Genmo, Z., C. Huaran, M. Shuqin, and Z. Deyuan (1995), Research on earthquakes induced by water injection in China, *Pure Appl. Geophys.*, *145*, 59–68.

Gomberg, J., and L. Wolf (1999), Possible cause for an improbable earthquake: The 1997 M_W4.9 southern Alabama earthquake and hydrocarbon recovery, *Geology*, *27*, 367–370.

Grasso, J.-R. (1992), Mechanics of seismic instabilities induced by the recovery of hydrocarbons, *Pure Appl. Geophys.*, *139*, 507–534.

Grollimund, B., M. D. Zoback, D. J. Wiprut, and L. Arnesen (2001), Stress orientation, pore pressure and least principal stress in the Norwegian sector of the North Sea, *Pet. Geosci.*, *7*, 173–180.

Grünthal, G. (Ed.) (1998), European Macroseismic Scale (EMS98), *Cah. Cent. Eur. Geodyn. Seismol.*, *15*, Cons. de l'Eur., Luxembourg.

Gupta, H. K., and R. K. Chadha (1995), Induced seismicity, *Pure Appl. Geophys.*, *145*(1), topical volume.

Havskov, J., and H. Bungum (1987), Source parameters for earthquakes in the northern North Sea, *Nor. Geol. Tidsskr.*, *67*, 51–58.

Havskov, J., and L. Ottemöller (2001), Seisan: The earthquake analysis software for Windows, Solaris and Linux, version 7.2, technical report, Inst. of Solid Earth Phys., Univ. of Bergen, Bergen, Norway.

Hettema, M., E. Papamichos, and P. Schutjens (2002), Subsidence delay: Field observations and analysis, *Oil Gas Sci. Technol.*, *57*, 443–458.

Hicks, E. C., C. D. Lindholm, and H. Bungum (2000), Stress inversion of earthquake focal mechanism solutions from onshore and offshore Norway, *Nor. Geol. Tidsskr.*, *80*, 235–250.

Kanamori, H. (1975), Theoretical basis of some empirical relations in seismology, *Bull. Seismol. Soc. Am.*, *65*, 1073–1095.

Kanamori, H. (1977), The energy release in great earthquakes, *J. Geophys. Res.*, *82*, 2981–2987.

Karnik, V., N. V. Kondorskaya, Y. V. Riznichenko, Y. F. Savarensky, S. L. Soloviev, N. V. Shebalin, J. Vanek, and A. Zapotek (1962), Standardisation of the earthquake magnitude scales, *Stud. Geophys. Geod.*, *6*, 41–48.

Kostrov, B. (1974), Seismic moment and energy of earthquakes, and seismic flow of rock, *Izv. Acad. Sci. USSR Phys. Solid Earth*, Engl. Transl., *1*, 23–40.

Kovach, R. L. (1974), Source mechanisms for Wilmington oil field, California, subsidence earthquakes, *Bull. Seismol. Soc. Am.*, *64*, 699–711.

Kvamme, L. B., R. A. Hansen, and H. Bungum (1995), Seismic-source and wave-propagation effects of *Lg* waves in Scandinavia, *Geophys. J. Int.*, *120*, 525–536.

Kvendseth, S. S. (1988), *Giant Discovery: A History of Ekofisk Through the First 20 Years*, Phillips Pet. Co., Norway.

Lienert, B. R., and J. Havskov (1995), Hypocenter 3.2: A computer program for locating earthquakes locally, regionally and globally, *Seismol. Res. Lett.*, *66*, 26–36.

Macbeth, C. D. (1988), Focal parameters of 31 March 1988, Ekofisk earthquake measured using waveform matching, *Tech. Rep. WL/88/22C*, Br. Geol. Surv., Edinburgh, U.K.

Maxwell, S. C., and T. I. Urbancic (2001), The role of passive microseismic monitoring in the instrumented oil field, *Leading Edge*, *20*, 636–639.

Maxwell, S. C., R. P. Young, R. Bossu, A. Jupe, and J. Dangerfield (1998), Microseismic logging of the Ekofisk reservoir, in *Eurock'98, SPE/ISRM Rock Mechanics in Pretroleum Engineering, Trondheim, Norway*, pp. 387–393, Soc. of Pet. Eng., Richardson, Tex.

McGarr, A. (1991), On a possible connection between three major earthquakes in California and oil production, *Bull. Seismol. Soc. Am.*, *81*, 948–970.

Nabelek, J., and G. Xia (1995), Moment-tensor analysis using regional data: Application to the 25 March, 1993, Scotts Mills, Oregon, earthquake, *Geophys. Res. Lett.*, *22*, 13–16.

Nagel, N. B. (1998), Ekofisk field overburden modelling, in *Eurock'98, SPE/ISRM Rock Mechanics in Pretroleum Engineering, Trondheim, Norway*, pp. 177–186.

Nagel, N. B. (2001), Compaction and subsidence issues within the petroleum industry: From Wilmington to Ekofisk and beyond, *Phys. Chem. Earth*, *26*, 3–14.

Nagel, N. B., and K. J. Strachan (1998), Implementation of cuttings reinjection at the Ekofisk field, in *Eurock'98, SPE/ISRM Rock Mechanics in Pretroleum Engineering, Trondheim, Norway*, pp. 95–103.

Nielsen, H. H. (2003), Reservoir and geoscience analysis of the 7th may 2001 seismic event in the Ekofisk area, technical report, ConocoPhillips, Tananger, Norway.

Nielsen, L., N. Balling, B. H. Jacobsen, and MONA LISA Working Group (2000), Seismic and gravity modelling of crustal structure in the Central Graben, North Sea: Observations along MONA LISA profile 3, *Tectonophysics*, *328*, 229–244.

Ottemöller, L., and J. Havskov (2003), Moment magnitude determination for local and regional earthquakes based on source spectra, *Bull. Seismol. Soc. Am.*, *93*, 203–214.

Pekot, L. J., and G. A. Gersib (1987), Ekofisk, in *Geology of the Norwegian Oil and Gas Fields*, edited by A. M. Spencer et al., pp. 73–87, Graham and Trotman, London.

Raleigh, C. B., J. H. Healy, and J. D. Bredehoeft (1972), Faulting and crustal stress at Rangely, Colorado, in *Flow and Fracture of Rocks*, *Geophys. Monogr. Ser.*, vol. 16, edited by H. C. Heard et al., pp. 275–284, AGU, Washington, D. C.

Scholz, C. H. (2002), *The Mechanics of Earthquakes and Faulting*, 2 ed., Cambridge Univ. Press, New York.

Segall, P. (1985), Stress and subsidence resulting from subsurface fluid withdrawal in the epicentral region of the 1983 Coalinga earthquake, *J. Geophys. Res.*, *90*, 6801–6816.

Segall, P. (1989), Earthquakes triggered by fluid extraction, *Geology*, *17*, 942–946.

Singh, S. K., R. J. Apsel, J. Fried, and J. N. Brune (1982), Spectral attenuation of *SH*-waves along the Imperial fault, *Bull. Seismol. Soc. Am.*, *72*, 2003–2016.

Sylte, J. E., L. K. Thomas, D. W. Rhett, D. D. Bruning, and N. B. Nagel (1999), Water induced compaction in the Ekofisk Field, paper SPE 56426 presented at the 1999 SPE Annual Technical Conference and Exhibition, Soc. of Pet. Eng., Houston, Tex.

Veith, K. F., and G. E. Clawson (1972), Magnitude from short period *P*-wave data, *Bull. Seismol. Soc. Am.*, *62*, 435–452.

Yerkes, R. F., and R. O. Castle (1976), Seismicity and faulting attributable to fluid extraction, *Eng. Geol.*, *10*, 151–167.

————————

K. Atakan and J. Havskov, Department of Earth Science, University of Bergen, Allegaten 41, Bergen, N-5007, Norway.

J. Braunmiller, Swiss Seismological Service, ETH-Hoenggerberg/HPP P 12.1, CH-8093 Zurich, Switzerland.

H. H. Nielsen, ConocoPhillips, P.O. Box 220, N-4056 Tananger, Norway.

L. Ottemöller, British Geological Survey, Murchison House, West Mains Road, Edinburgh EH9 3LA, UK. (lot@bgs.ac.uk)